Journal of Catalysis 292 (2012) 239–245

Contents lists available at SciVerse ScienceDirect

Journal of Catalysis

journal homepage: www.elsevier.com/locate/jcat

Aqueous Phase Reforming of ethylene glycol – Role of intermediates in catalyst performance

D.J.M. de Vlieger, B.L. Mojet, L. Lefferts, K. Seshan *

Catalytic Processes and Materials (CPM), MESA+ Institute, Faculty of Science and Technology, University of Twente, P.O. Box 217, 7500 AE Enschede, The Netherlands

ARTICLE INFO

Article history:
Received 22 February 2012
Revised 27 April 2012
Accepted 27 May 2012
Available online 29 June 2012

Keywords:
Boehmite
Raman
FTIR spectroscopy
Deactivation
Acetic acid
Sustainable

ABSTRACT

Liquid product formation during the aqueous catalytic reforming of ethylene glycol (EG) was studied up to 450 °C and 250 bar pressure. Methanol, ethanol, and acetic acid were the main liquid by-products during EG reforming in the presence of alumina-supported Pt and Pt–Ni catalysts. The effect of these by-products on selectivity and catalyst stability was further investigated by studying reforming of these components. Reforming of these products was shown to be responsible for the formation of alkanes. The high dehydrogenation activity of Pt–Ni catalysts leads to high H_2 yields during EG reforming by (i) suppressing the formation of methane during methanol reforming (a major by-product of EG reforming) and (ii) suppressing the formation of acetic acid. In addition, the decrease in acetic acid formation showed a positive effect on catalyst lifetime. Acetic acid was found to be responsible for hydroxylation of the Al_2O_3 support, leading to migration and coverage of the metal particles by $Al(OH)_x$ and resulting in deactivation of the Pt-based catalysts.

1. Introduction

In the future, hydrogen from renewable resources is projected to replace fossil fuels, at least partly, to help reduce anthropogenic CO_2 emissions [1]. A widely studied process for the production of 'green' hydrogen is reforming of oxygenates, for example alcohols, acids or aldehydes [2,3]. Such oxygenates appear in waste streams of food and other bio-based processes, for instance, the aqueous fraction of biomass pyrolysis oil is one such example. Typical concentrations of oxygenates in these streams are up to ±20 wt% [4].

One way to generate hydrogen from these components is conventional steam reforming followed by water gas shift reaction. These process steps are energy intensive because (i) they are usually carried out at high temperatures (600–700 °C) [5] and (ii) in the case of aqueous waste streams, it requires evaporation of the large amounts of the water present [6]. Dumesic and co-workers [2] tackled this problem by developing the Aqueous Phase Reforming (APR) process by keeping water in the liquid phase by exerting increased pressures. This process is typically carried out in the range of 175–265 °C and 34–56 bar. Thermodynamics favor hydrogen at these low temperatures, but the reaction rates are slow [7]. Increasing the temperature to obtain commercially viable reaction rates has the disadvantage of increased formation of undesired alkanes [8], thus reducing the hydrogen yield.

Many studies on the catalytic reforming of model oxygenates under APR conditions have been reported recently [9–13]; ethanol, ethylene glycol, glycerol are typical examples. Information on mechanistic sequences that take place during APR is limited, and in the case of ethylene glycol (EG), Dumesic et al. [13] suggested that reforming is initiated *via* dehydrogenation and formation of an adsorbed oxygenate (acetylinic dialcohol type) intermediate. In a desired sequence, C–C bond cleavage and subsequent water gas shift leads to CO_2 and H_2. However, rearrangement/desorption of the oxygenate intermediate leads to acids and/or one C–O bond scission to formation of alcohols. Sequential reforming of acids and alcohols often cause formation of alkanes as by-products. In addition, direct hydrogenation of CO_x formed can also give CH_4 or higher alkanes through the Fischer–Tropsch reaction [13]. These parallel routes lower the hydrogen yield, which is a serious drawback.

Deactivation and catalyst instability are other issues during APR. Activity loss during APR is often associated with loss of catalytic sites (leaching, sintering) or blockage by carbonaceous species, but specific details are not available in literature. However, in the case of high temperature gas-phase steam reforming of oxygenates, reasons for catalyst deactivation were identified [14–20]. For example, coke deposition caused by oligomerization of olefins formed was reported to be an issue during steam reforming of ethanol [14,15]. Formation of unsaturated C_xH_y species *via* dehydrogenation reactions is often proposed as a precursor to coke [16–18]. We have shown earlier that acetic acid is converted to acetone during steam reforming, which further reacts to form coke precursors

* Corresponding author.
E-mail address: k.seshan@utwente.nl (K. Seshan).

0021-9517/$ - see front matter © 2012 Elsevier Inc. All rights reserved.
http://dx.doi.org/10.1016/j.jcat.2012.05.019

such as mesityl oxide or mesitylene [19]. The product CO can also disproportionate exothermically to form carbon through the Boudouard reaction ($2CO \rightarrow CO_2 + C$) [20].

We reported recently that Pt/Al_2O_3 catalyst showed conversion rates for APR of ethylene glycol that are very attractive for industrial application [8]. However, this catalyst was found to deactivate during the reaction. Pt/Al_2O_3 also gave lower H_2 selectivity due to the formation of alkanes. We showed further that the presence of Ni in the Pt/Al_2O_3 catalyst suppressed the above problems such as catalyst deactivation and high amounts of alkane formation and provided the basis for the development of an efficient catalyst [8].

In this study, the role of intermediates that are formed during aqueous reforming of ethylene glycol on the formation of alkanes is studied. Further, the reason for the loss of activity is investigated in relation to intermediates formed during reactions. Correlations thus drawn are discussed in relation to the promotion of Pt/Al_2O_3 with Ni. Improving catalyst stability and at the same time enhancing hydrogen selectivity at the expense of alkanes for the reforming of ethylene glycol is essential in the design of an efficient APR catalyst.

2. Experimental

2.1. Catalyst preparation and characterization

Experimental details regarding catalyst preparation and characterization are discussed Table 1: Characterictics of the studied catalystsin a previous publication [8]. Details of the catalysts used for this study are summarized in Table 1. Metal loadings were determined using a Philips X-ray fluorescence spectrometer (PW 1480). Pt metal particle size was both determined by CO-chemisorption and TEM imaging. FT-IR (Bruker Tensor 27, 4 cm^{-1} resolution with 64 scans, range between 600 and 4000 cm^{-1}, 5 mm aperture) and Raman (Bruker Senterra, laser wavelength 532 cm^{-1} with 10 mW power, 3–5 cm^{-1} resolution and range between 65 and 4000 cm^{-1}) spectra were recorded at room temperature for fresh and used catalysts.

2.2. Catalytic testing

The experimental setup used is described in detail in an earlier publication [8]. A 2 mL min^{-1} flow of 1 wt% oxygenate solution (ethylene glycol (⩾99.9%, Sigma–Aldrich), acetic acid (⩾99.9%, Merck), or methanol (⩾99.9%, Merck), or ethanol (⩾99.9%, Merck)) was first preconditioned to the operating conditions (275 °C and 200 bar) before it entered the reactor in which 1.0 g of catalyst was placed. The reforming reactions were studied during 5-h time-on-stream. The reactor effluent was separated into gas and liquid products. An online Shimadzu TOC-VCSH analyzer determined carbon concentrations in the feed solution and the liquid effluent. TOC analyses of the liquid phases are subjected to a relative error of 1%. A Shimadzu HPLC was used to identify the liquid products formed during the reforming reactions. The HPLC was equipped with a RID-10A detector and an Aminex HPX-87H (300 × 7.8 mm) column. An aqueous solution of 0.005 M H_2SO_4 was used as elutant phase and was flown at a rate of 0.600 mL min^{-1}. The column was operated at 35 °C. Sample volumes of 20 μL were injected onto the column. Gas analysis was carried out with a Varian CP-4900 Micro GC using MS5 and PPQ columns. Relative errors of maximum 2% were introduced by the GC measurements.

Table 1
Characteristics of the studied catalysts [8].

Catalyst	Metal loading by XRF (wt%)	Average metal particle size (nm)	BET surface area (m^2/g)
γ-Al_2O_3	–	–	200
Pt/γ-Al_2O_3	1.45	⩽1 (TEM) 1.6 (CO-chemisorption)	198
Pt–Ni/γ-Al_2O_3	1.15 Pt–0.35 Ni	⩽1 (TEM)	198

2.3. Definitions of conversion and selectivity

In this paper, carbon-to-gas conversion is defined as the percentage of carbon in the feed that is transformed to carbon in gaseous products (CO_x, hydrocarbons). Carbon removed from the liquid phase can either go to gas phase products or coke. Determining the amount of carbon in gas could be done by combining the GC results and gas production results. The ideal gas law can then be applied to calculate the moles of carbon in the gas phase. This method contains many parameters and assumptions that compromise its accuracy. If coke formation does not occur, as was the case for this study, then all carbon removed from the liquid phase gasified. The carbon content in liquid streams can be determined very accurately (relative error <1%) by the TOC analyzer, and therefore, the following expression was used to calculate carbon to gas conversion $\frac{\text{“moles C”}_{Feed} - \text{“moles C”}_{Reactor\ liquid\ effluent}}{\text{“moles C”}_{Feed}} \times 100\%$.

Selectivity to carbon containing gas phase products ($i = CO_x$, CH_4 and C_2+) was calculated according to $selec.i\% = \frac{\text{“moles C”}\ in\ species\ i}{\text{“moles C”}\ in\ gas\ phase} \times 100\%$. Side-reactions leading to carbon containing molecules in the liquid phase were not taken into account in these selectivity calculations.

3. Results and discussion

3.1. APR of ethylene glycol

Reforming of aqueous bio-organic streams is only interesting for industrial applications when feeds with high oxygenate concentrations (>15 wt%) can be used. However, larger concentrations of intermediates and products formed under these conditions can lead to extensive secondary reactions. Thus, two sets of reforming experiments were carried out: (1) 20 wt% ethylene glycol (EG) solution was studied in supercritical water (450 °C and 250 bar) and (2) a 1 wt% EG solution was studied at similar conversions obtained by using milder reaction conditions (275 °C and 200 bar). The obtained results are shown in Table 2. Conversion to gas- and liquid-phase products is mentioned separately in Table 2 to allow a good comparison of the gasification efficiency. Total EG conversion to liquid and gas products was ±90% for both reactions with the remaining carbon being unconverted EG. Carbon balances were complete within an error margin of 5%. It can be seen that at the higher EG concentration and higher temperature, the amount of carbon containing products in the liquid phase increased. Alkane formation is also higher under these conditions. The alkane formation was much lower in the experiment with 1 wt% EG. In both cases, componential HPLC analysis of the liquid reactor effluent showed that (in addition to unconverted EG) three other main components were present in the reactor effluent. These were acetic acid, methanol, and ethanol.

As discussed previously, components such as acids and alcohols are often suggested as precursors for the formation of alkanes. Further, we also stated that the addition of Ni to Pt/Al_2O_3 suppressed the formation of alkanes during reforming of EG [8]. In order to probe the role for Ni, a detailed componential HPLC analysis of the liquid reactor effluents of 1 wt% EG reforming (275 °C and 200 bar) in the presence of Pt or Pt–Ni catalysts was carried out. The results are shown in Fig. 1. It is seen from Fig. 1 that the reactor

Table 2
Conversions and alkane selectivities for ethylene glycol reforming under different conditions in the presence of 1.5 wt% Pt/Al_2O_3.

EG (wt%)	Reaction Temp. (°C)	Reaction Press. (bar)	WHSV (h^{-1})	Conversion to gas (%)	Conversion to liquid (%)	Alkanes in gas (%)
20	450	250	12	74	15.4	16.9
1	275	200	1.2	78	11.7	0.3

effluent in presence of the Ni-promoted catalyst showed the same by-products (acetic acid, methanol, and ethanol). The concentrations of methanol and ethanol in the reactor effluent were not influenced significantly by the presence of Ni. However, the concentration of acetic acid was found to be three times lower for the Ni-promoted catalyst.

At this point, it is useful to recall the mechanistic sequences proposed in the literature for the aqueous phase reforming of EG by Dumesic et al. [13]. It is suggested, without experimental evidence, that dehydrogenation of EG over Pt is the first step in the reforming pathway. During this step, the hydrogen atoms from the hydroxyl groups are removed by O–H cleavage on the Pt surface [21]. In an optimal situation, the resulting adsorbed ·O–CH_2–CH_2–O· species is further dehydrogenated and undergoes C–C cleavage to form adsorbed CO [21]. The adsorbed intermediate species ·O–CH_2–CH_2–O· can also undergo rearrangement over the acidic γ-Al_2O_3 support to form acetic acid [13]. However, in another study, we also observed the formation of acetic acid during APR of EG using a carbon-supported Pt catalyst [22]. The chemical inertness of this type of support material excludes the rearrangement of ·O–CH_2–CH_2–O· over the support to form acetic acid. The ionic nature of hot compressed water is reported to catalyze organic reactions in the aqueous phase, such as the Cannizzaro reaction [23] and isomerization reactions [24]. As discussed later in this manuscript, the Cannizzaro-derived reaction is not a dominant contributor to acetic acid formation. The isomerization reaction (either catalyzed by the support or by the ions from the liquid water) of adsorbed ·O–CH_2–CH_2–O· is responsible for the majority of acetic acid formed.

Competition between dehydrogenation and isomerization of adsorbed ·O–CH_2–CH_2–O· dictates the relative formation of hydrogen and acetic acid. Dehydrogenation will be catalyzed by metals (Pt, Ni), and isomerization would be assisted by an acidic oxide (in this case γ-Al_2O_3).

The role of Ni in the suppression of acetic acid formation (Fig. 1) can be inferred from DFT calculations that predicted "increased" binding energies for adsorbed species derived from ethylene glycol on the surface monolayer Ni–Pt (1 1 1) as compared to Pt (1 1 1) [21]. We suggest that the increased binding energies of the oxygenate intermediates lead to longer residence times on the metal and result in increased dehydrogenation activity. It would be useful to estimate the energetics for the two routes (dehydrogenation *vs.* isomerization) on Pt and Pt–Ni bimetallic surfaces by theory, but that is beyond the scope of the current study. In addition, the dissociation of the O–H bond is suggested to be the rate-limiting step in the conversion of ethylene glycol [21]. The higher dehydrogenation activity of the Pt–Ni catalyst results in faster dehydrogenation of the O–H groups and hence a higher overall reforming rate. This is in agreement with earlier studies [8,25] where Pt–Ni/Al_2O_3 catalysts showed higher conversions for the reforming of ethylene glycol than Pt/Al_2O_3.

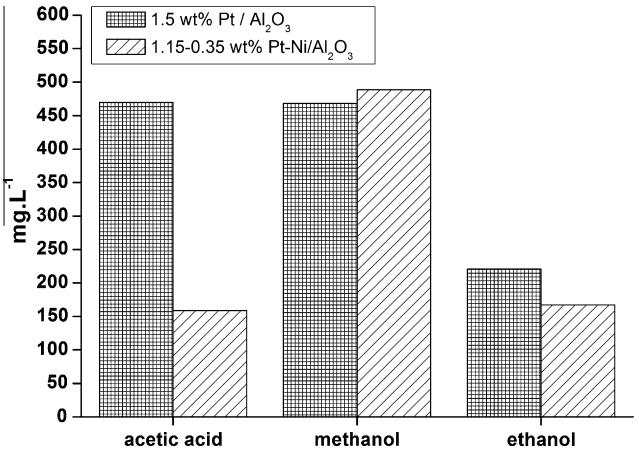

Fig. 1. Liquid by products during catalytic reforming of 1 wt% ethylene glycol at 275 °C and 200 bar (WHSV = 1.2 h^{-1}). Results for Pt and Pt–Ni catalysts showed conversions to gas phase of 78% and 88%, respectively.

3.2. APR of model components

Aqueous phase reforming experiments with liquid products formed during the APR of EG was carried out using individual components (Fig. 2). Reforming experiments (with acetic acid, methanol, ethanol) were conducted at 275 °C and 200 bar in the presence of Pt/Al_2O_3 or Pt–Ni/Al_2O_3. Feed concentrations of 1 wt% were used so as to work in the same concentration range as the liquid by-products formed during EG-reforming experiments. For example, a total conversion of 15% to methanol, ethanol and acetic acid was observed during the reforming of 20 wt% EG (Table 2), resulting in a total concentration of 3 wt% liquid by-products. As the three were in the same range, concentration of each was fixed at 1 wt% for further experiments.

Blank reforming experiments (275 °C and 200 bar) with methanol, ethanol, and acetic acid without catalysts showed conversions below 5%. In the presence of Pt/Al_2O_3 and Pt–Ni/Al_2O_3 catalysts, conversions were in the range of 50–80% (Fig. 2). For methanol, the conversion was around 60% (Fig. 2A) and for ethanol higher, ±80% (Fig. 2B). The higher reforming activity of ethanol on both catalysts may be related to the reforming sequences that take place. The initial step in the reforming of aliphatic alcohols involves the dissociation of the O–H bond resulting in adsorbed methoxy or ethoxy species on the Pt surface [26,27]. Similar dissociation energies are reported [28] for breaking the O–H bond in these alcohols and can therefore not be responsible for the difference in reforming activity. During reforming of alcohols, hydrogen formation requires the formation of adsorbed carbon monoxide which can undergo WGS to form H_2 and CO_2. In the case of methanol to form CO, it is necessary for the adsorbed methoxy species to undergo three C–H bond cleavages. For ethanol, the adsorbed ethoxy species must undergo two C–H and one C–C bond cleavage. Further it was suggested that the cleavage of the C–C bond in ethanol leads to an adsorbed methyl species [27]. We speculate that the different routes to decompose the alcohols may be the reason for the observed difference in reactivity. For the reforming of acetic acid (Fig. 2C), initial conversion levels of ±50% were obtained. However, the conversion decreased rapidly with time for both the Pt and Pt–Ni catalysts, this will be discussed later on in the manuscript.

3.3. Alkane formation during APR

The formation of alkanes during the catalytic reforming of acetic acid, methanol and ethanol are shown in Fig. 3. The selectivity toward alkanes (mainly methane) was found to be the highest

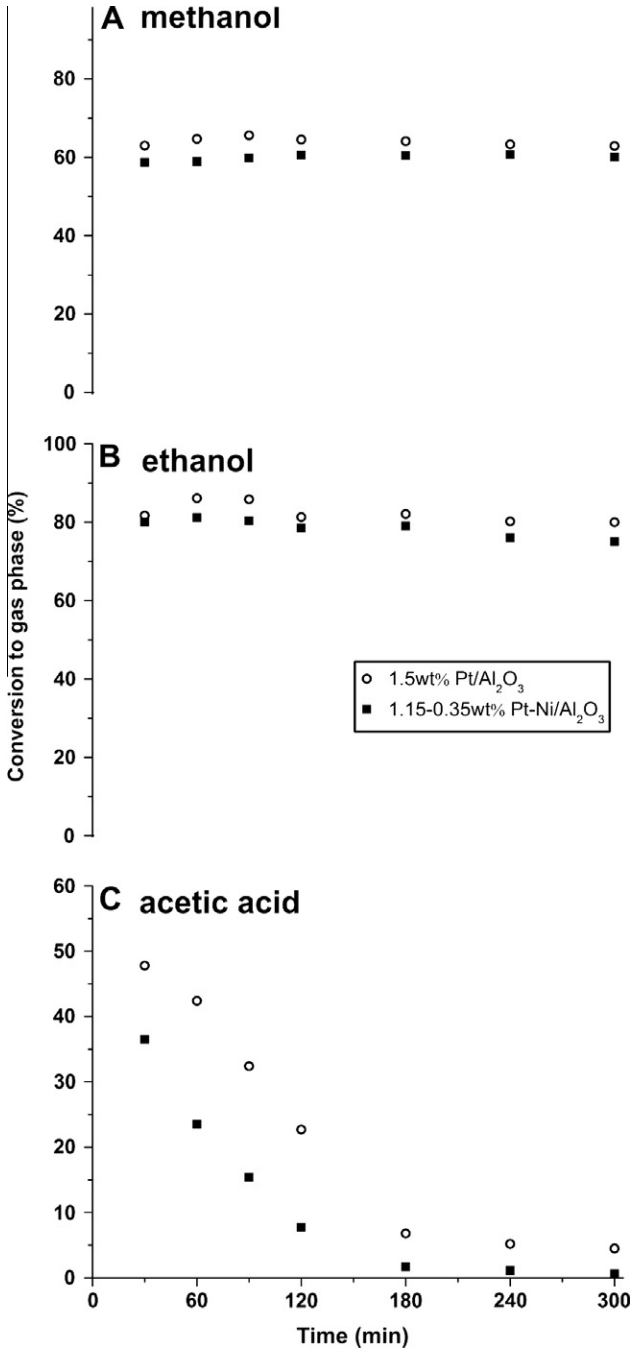

Fig. 2. Conversion to gas phase for reforming (275 °C and 200 bar) of 1 wt% methanol (A), ethanol (B), or acetic acid (C) using 1.5 wt% Pt/Al_2O_3 (○) and 1.15–0.35 wt% $Pt–Ni/Al_2O_3$ (■) catalysts.

(±47%) during acetic acid reforming. For the reforming of methanol, a selectivity of 8% toward CH_4 was observed for the Pt catalyst. In the case of ethanol reforming, the Pt catalyst showed a CH_4 selectivity of ±20%. The higher amounts of methane observed during ethanol reforming is attributed probably to the CH_x fragment formed by C–C bond breaking of ethanol [26] on the Pt surface. CH_x fragments can recombine with adsorbed H atoms on the Pt surface to form methane. A similar sequence is also suggested for acetic acid on Pt-based catalysts [19,29]. In the case of methanol, C–O bond breaking is necessary to generate these adsorbed CH_x species that lead to the production of methane. High C–C bond–breaking activities for Pt during the reforming of ethanol and low

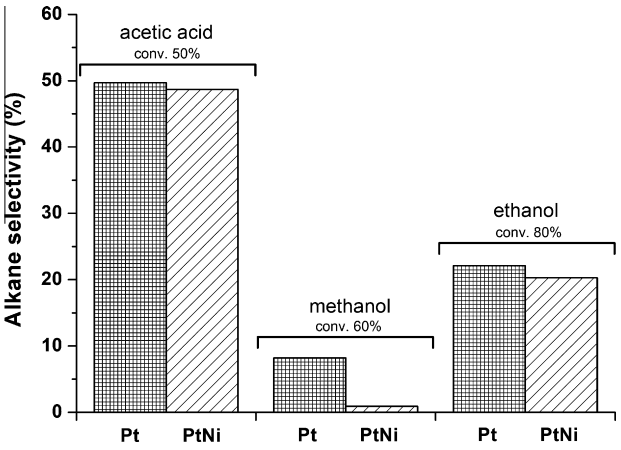

Fig. 3. Formation of alkane during the catalytic reforming of 1 wt% acetic acid, methanol, and ethanol at 275 °C and 200 bar. Conversions to gas phase (conv.) are mentioned in the Figure.

activity for C–O bond breaking [13] during the reforming of methanol can explain the observed differences for methane formation.

For methanol reforming with the Pt–Ni catalyst, almost no methane was formed (Fig. 3). Methanol was found to be one of the major products during the reforming of EG (Fig. 1) that explains why $Pt–Ni/Al_2O_3$ catalyst shows almost no methane formation in agreement with earlier studies [8,25]. The lower methane production observed during methanol reforming in the presence of Pt–Ni can be explained by the enhanced dehydrogenation activity of Pt–Ni catalyst [21], favoring C–H cleavage instead of C–O cleavage in methanol. Promoting the Pt catalyst with Ni did not affect the alkane (methane) selectivity for acetic acid or ethanol reforming as can be expected from the reforming routes. Reforming of these compounds inherently lead to CH_3 species on the catalyst surface, which is a precursor for methane formation. In case of methanol reforming, the intermediate CH_3O must undergo C–O cleavage to form CH_3 (and hence methane). Methane formation during methanol reforming can be prevented by avoiding C–O cleavage.

3.4. Catalyst deactivation

Reforming experiments with 1 wt% methanol (Fig. 2A) and ethanol (Fig. 2B) solutions showed stable activity levels for both Pt and Pt–Ni catalysts. Catalysts used for acetic acid reforming deactivated during the reaction (Fig. 2C). Both catalysts showed similar deactivation rates. The catalysts lost all activity after 3 h on stream with final conversion levels (5%) being similar to the reforming experiment without a catalyst.

Deactivation of the catalyst with acetic acid is commonly observed in reforming reactions [19]. The formation of methane resulting from acetic acid decomposition is reported in literature to be a possible cause for the deactivation of catalysts [30]. It is suggested that C–H bond breaking in methane further results in CH_x species ($1 \leqslant x \leqslant 2$) on the catalytic surface. These fragments can further oligomerize to coke species [19]. However, catalysts used for ethanol reforming were found to be stable while also producing high amounts of methane (20%). It is also known that Pt and Ni catalysts are stable for the reforming of methane. Therefore, it is concluded that methane-induced deactivation is unlikely, and the dominant deactivation pathway is due to other causes.

Further, liquid products formed during the APR of acetic acid, methanol, and ethanol were determined to find any role for them in catalyst deactivation. During acetic acid reforming, a conversion of 7% to liquid by-products was observed for the Pt catalyst. By-

products were identified as formaldehyde and iso-propanol. For ethanol, a conversion of ±6% to liquid by-products was found for the Pt catalyst. The main product was acetic acid, and the remaining was acetaldehyde (<0.5%). The Cannizzaro reaction could be responsible for some of the acetic acid formed during ethanol reforming. The Pt and Pt–Ni catalysts studied did not influence the amount of acetic acid, and acetaldehyde formed during ethanol reforming, while during EG reforming, the amount of acetic acid was strongly dependent on the type of catalyst. This shows that the Cannizzaro-derived reaction is not a dominant contributor to acetic acid formation during EG reforming.

No liquid by-products were observed during methanol reforming. Interestingly, the presence of Ni in the Pt–Ni catalyst did not show any significant differences on the type or amount of secondary liquid by-products during the reforming of acetic acid, methanol, or ethanol compared to the mono-metallic Pt catalyst. No apparent conclusions can thus be derived from these experiments.

In the case of the Pt/Al_2O_3 catalyst that deactivated during acetic acid reforming, CO-chemisorption experiments showed a Pt dispersion of only 0.03% (fresh catalyst 67%), indicating that almost all accessible Pt surface area was lost. Loss of catalytic metal by leaching, metal particle growth by sintering and coke formation are common causes for the loss of catalytic surface and hence the deactivation of catalysts. XRF elemental analysis of the deactivated Pt/Al_2O_3 catalyst used for acetic acid reforming showed that no Pt was lost by leaching from the catalyst. Sintering is a thermo-physical effect and therefore dictated by the operating conditions (temperate and pressure). Catalyst stability was not affected during the reforming of methanol and ethanol when the reaction was performed at the similar operating conditions as for acetic acid reforming, thus excluding sintering as cause of catalyst deactivation. The formation of coke on the surface of Pt based catalysts during steam reforming of acetic acid is often reported [19]. Carbon deposits on the deactivated Pt/Al_2O_3 catalyst that was used for aqueous reforming of acetic acid was studied by TGA-MS up to a temperature of 800 °C in oxygen (1 v/v% O_2 in N_2). No weight loss attributed to the removal of carbonaceous deposits was observed during the experiment, indicating that carbonaceous deposits were not present on the catalyst. IR and Raman experiments (discussed below) also did not show presence of any carbonaceous species. In addition, the regeneration of the deactivated Pt catalyst used for acetic acid reforming was attempted by oxygen treatment (up to 500 °C), but the treated catalyst did not regain the activity for the reforming of EG. Based on these results, carbonaceous deposits as cause for catalyst deactivation can also be ruled out. Under conventional gas-phase-reforming conditions, it is well accepted that steam reforming of acetic acid can lead to coke formation via intermediates involving acetone, diacetone alcohol, and mesitylene [19,31,32]. Hot-compressed water has a high tendency to dissolve organic species, including carbonaceous deposits [3,33]. Carrying out reforming in hot-compressed water therefore plays an important role in keeping the catalytic surface clean of any coke deposits that prevent accessibility of oxygenates to catalytic sites.

Raman spectroscopy was used to study spent Pt catalysts used for reforming of methanol, acetic acid, and water only (blank experiment). Raman spectra were taken at room temperature in air. The obtained spectra are shown in Fig. 4. The spectra were normalized based on the most pronounced Raman band at 362 cm^{-1} for easy comparison. In all three cases, Raman spectra of the used catalysts showed five sharp adsorption bands in the range of 65–4000 cm^{-1}. These bands are attributed to Boehmite [34,35], which is formed as a result of the phase change of the γ-Al_2O_3 support in our catalyst when subjected to hot-compressed water [8,36]. The three bands at 362, 494, and 672 cm^{-1} are attributed to vibrational modes of the Boehmite Al–O bond [34]. The two other adsorption bands, located at 3212 and 3076 cm^{-1}, are attributed to stretching

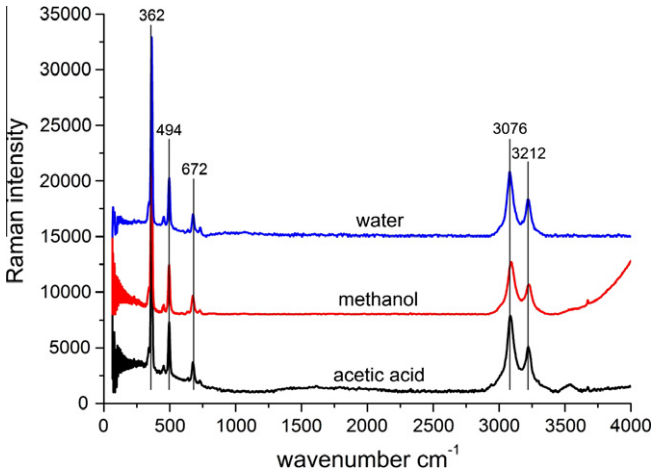

Fig. 4. Raman spectra of spent 1.5 wt% Pt/Al_2O_3 catalysts used for reforming (275 °C and 200 bar) of acetic acid, methanol, and water only.

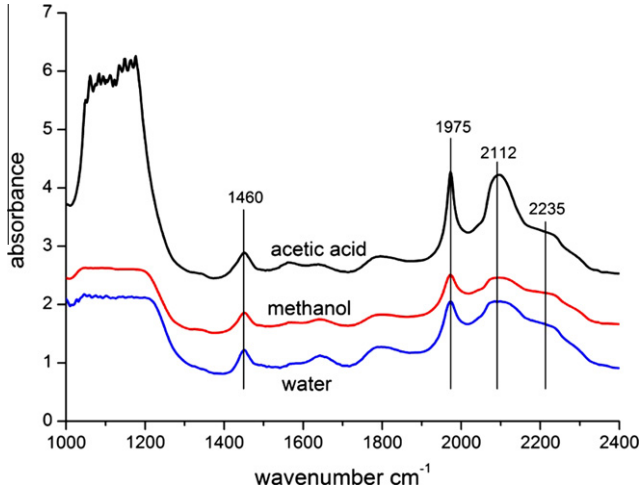

Fig. 5A. FT-IR spectra of spent 1.5 wt% Pt/Al_2O_3 catalysts used for the reforming (275 °C and 200 bar) of acetic acid, methanol, and water only.

vibrations of O–H bonds [34]. A weak band at 3565 cm^{-1} is visible in the spectra of the acetic acid reforming catalyst, and this band can be attributed to hydroxyl groups with a higher acidity. Interestingly, the ratio between the normalized bands at 362 cm^{-1} and the OH bands at 3076 and 3212 cm^{-1} show clearly that more hydroxyl species are present in case of the deactivated Pt catalyst compared with the active catalysts.

The differences in hydroxyl groups and the cause for deactivation of the Pt catalyst were further investigated by Fourier-Transformed Infrared spectroscopy (FT-IR). FT-IR spectra of spent Pt catalysts were taken at room temperature in air. Spectra were normalized for sample weight and are shown in the frequency range of 1000–2400 cm^{-1} in Fig. 5A. No information could be derived from the IR spectrum above 2400 cm^{-1} due to the broad and intensive molecular water band that covered the whole range up to the maximum of 4000 cm^{-1}. For all catalysts, a broad band in the frequency region 1000–1200 cm^{-1} was observed which can be assigned to the Al–OH bending vibrations in the Boehmite crystal structure [35]. Multiple weak bands are observed in the region 1300–1900 cm^{-1}, and these are attributed to different kinds of adsorbed carbon pollutants (i.e., CO_2 adsorption from air leading to surface carbonates) and water adsorption. Two strong bands appeared at 1975 and 2112 cm^{-1}, and these have been suggested to originate from complex Al–O–H zigzag structures in Boehmite [35].

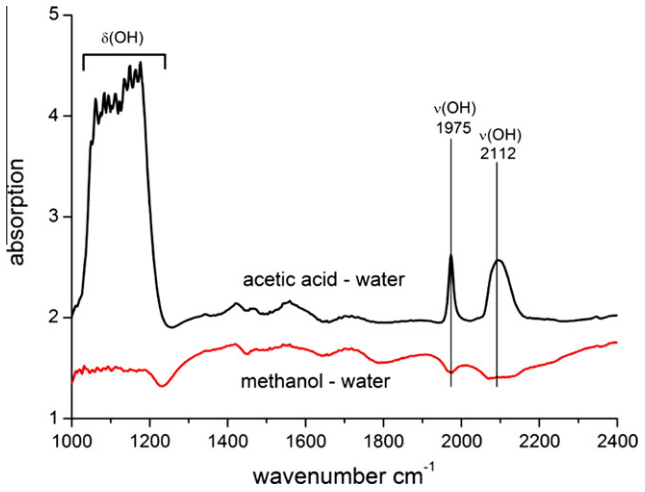

Fig. 5B. Difference FT-IR spectra of spent Pt catalysts.

FT-IR spectra of the spent catalysts were subtracted from each other as shown in Fig. 5B to study the differences in chemical groups on the surfaces of the used Pt catalysts. Subtracting the spectrum of the catalyst that was exposed to water only from that of aqueous methanol solution resulted in a more or less flat line, indicating that the surface composition of the active catalysts (used for methanol and water only) are similar. Subtracting the spectrum of the catalyst subjected to only water from the spent deactivated acetic acid catalyst resulted in 3 strong bands; one lattice vibration in the region 1000–1200 cm^{-1} and two sharp OH related bands located at 1975 and 2112 cm^{-1}. Also in the Raman spectra, the acetic acid treated sample showed the highest O–H intensity (Fig. 4). These results indicate the presence of a highly hydroxylated type of Boehmite in the acetic acid deactivated catalyst compared with the active catalyst used in methanol APR.

A cause for the deactivation of the catalyst can be inferred from the increased number of hydroxyl groups. It is known that the stability of the Al_2O_3 surface strongly depends on the pH of the medium [37]. Acids are reported to cause dissolution of Al_2O_3 [38], and this is an important process that can affect catalyst properties. The dissolution rate of metal oxide supports increases at lower pH values and involves protonation of Al–O–Al bonds to form Al–OH. Further protonation and/or rearrangement of oxide ligands are responsible for the dissolution of Al_2O_3 [38]. The increase in hydroxyl groups on the surface of the catalysts used for acetic acid reforming indicates that the surface structure of Al_2O_3 is affected by acetic acid. Dissociation constants for acids are much higher in hot-compressed water compared with normal water [33], and therefore, we propose that acetic acid behaves as a stronger acid in hot-compressed water resulting in protonation and sequential leaching of the alumina surface. In hot-compressed water, where solubility of inorganic oxide materials is low, it can be expected that hydroxylated alumina that leached off can be re-deposited on the catalyst. Fig. 6 shows the TEM image of the Pt-deactivated catalyst. The Pt particle and the lattice distances of the Al_2O_3 are clearly visible. The Al_2O_3 lattice distance is measured in the picture to be 0.7 nm. The Pt particle is covered by a layer that shows the same lattice distances of 0.7 nm as alumina, indicating that the Pt is covered by alumina. From these results, we conclude that the cause of deactivation of the Pt catalyst is coverage of catalytic Pt sites by hydroxylated alumina layer.

Although the exact mechanism responsible for coverage of the Pt particle by alumina is not yet known, we show here that this mechanism likely involves hydroxylation of the γ-Al_2O_3 support and is propagated by a strong acidic environment, resulting from the high proton dissociation of acids in hot-compressed water.

3.5. Reaction pathways

The reaction pathways involved in the reforming of ethylene glycol proposed by Dumesic et al. [13] have been adapted with the new insights obtained from this study. The resulting-extended reaction sequences are proposed in Fig. 7. Modifications include formation of methanol from ethanol and deactivation by acetic acid. We have identified methanol as an important liquid by-product. Methanol can be formed during the reforming of ethanol as a result of C–C bond cleavage. Reforming of methanol can either lead to methane or to hydrogen, and the preferential route is controlled by the dehydrogenation activity of the catalyst. The formation of acetic acid, ethanol, and methanol during the reforming of EG is considered undesired because consecutive reactions involving these compounds are responsible for the formation of alkanes (mainly methane). In addition, the presence of acetic acid can cause the deactivation of the catalyst. The formation of liquid by-products and alkanes mainly result from C–O bond cleavage, dehydration, and hydrogenation reactions. The pathway to high hydro-

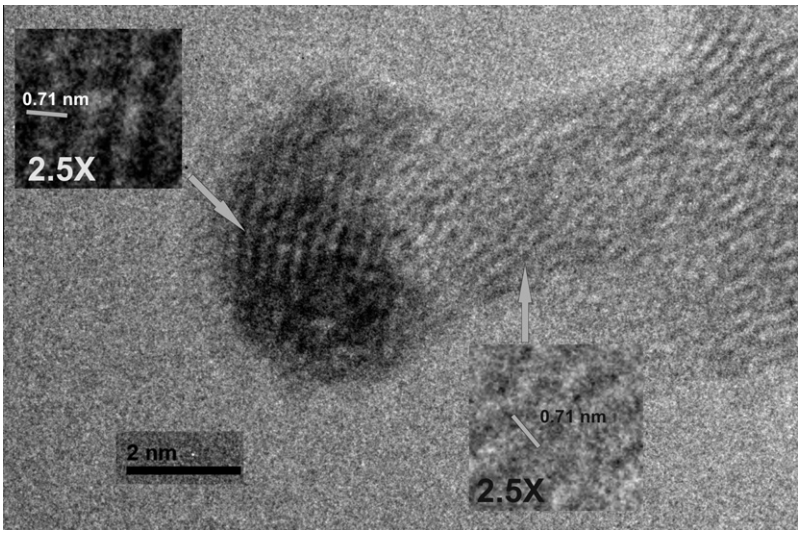

Fig. 6. TEM image of an alumina covered Pt particle.

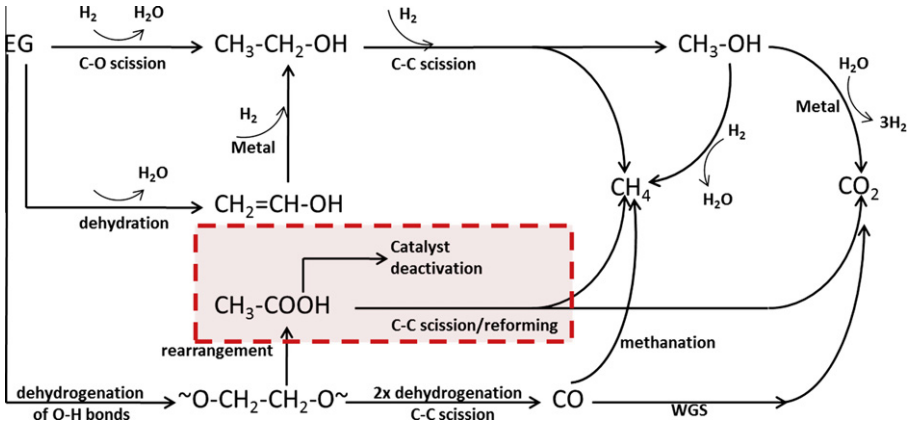

Fig. 7. Schematic representation of modified reaction pathways during aqueous reforming of ethylene glycol.

gen yields involves dehydrogenation of ethylene glycol. Competition between dehydrogenation and isomerization of the adsorbed intermediate to acetic acid determines the selectivity toward alkanes (and hence H_2 yields). Addition of Ni to alumina-supported Pt catalysts increased the dehydrogenation activity. As a consequence, a decrease in the formation of alkanes and improved stability was accomplished by suppressing acetic acid formation.

4. Conclusions

We identified methanol, ethanol, and acetic acid as the main liquid by-products during the reforming of ethylene glycol in hot-compressed water in the presence of Al_2O_3-supported Pt and Pt–Ni catalysts. Side-reactions involving these liquid by-products lead to the formation of high amounts of methane. Acetic acid was shown to be responsible for the deactivation of Pt and Pt–Ni catalysts by hydroxylation of the Al_2O_3 surface. Re-deposition of the dissolved alumina on the catalyst leads to the blocking of catalytic Pt sites and hence the deactivation of the catalyst. The increased dehydrogenation activity of the Pt–Ni catalyst was found to suppress the formation of acetic acid during ethylene glycol reforming and thereby increasing the H_2 selectivity and catalyst lifetime.

Acknowledgments

This project was supported by ACTS (Project Number 053.61.023). The authors greatly acknowledge Ing. Louise Vrielink for BET and XRF analysis, Dr. Rico Keim for TEM-EDX imaging, Karin Altena for dispersion measurements, Ing. Benno Knaken and Ing. Bert Geerdink for technical support.

References

[1] A. Tanksale, J.N. Beltramini, G.M. Lu, Renew. Sustain. Energy Rev. 14 (2010) 166.
[2] R.D. Cortright, R.R. Davda, J.A. Dumesic, Nature 418 (2002) 964.
[3] Y. Guo, S.Z. Wang, D.H. Xu, Y.M. Gong, H.H. Ma, X.Y. Tang, Renew. Sustain. Energy Rev. 14 (2010) 334.
[4] L. Garcia, R. French, S. Czernik, E. Chornet, Appl. Catal. A 201 (2000) 225.
[5] S. Adhikari, S. Fernando, F. To, R. Bricka, P. Steele, A. Haryanto, Energy Fuel 22 (2008) 1220.
[6] E.C. Vagia, A.A. Lemonidou, Int. J. Hydrogen Energy 32 (2007) 212.
[7] R.R. Davda, J.A. Dumesic, Angew. Chem. Int. Ed. 42 (2003) 4068.
[8] D.J.M. de Vlieger, A.G. Chakinala, L. Lefferts, S.R.A. Kersten, K. Seshan, D.W.F. Brilman, Appl. Catal. B 111–112 (2012) 536.
[9] J.W. Shabaker, G.W. Huber, J.A. Dumesic, J. Catal. 222 (2004) 180.
[10] A.O. Menezes, M.T. Rodrigues, A. Zimmaro, L.E.P. Borges, M.A. Fraga, Renew. Energy 36 (2011) 595.
[11] B. Roy, K. Loganathan, H.N. Pham, A.K. Datye, C.A. Leclerc, Int. J. Hydrogen Energy 35 (2010) 11700.
[12] A. Wawrzetz, B. Peng, A. Hrabar, A. Jentys, A.A. Lemonidou, J.A. Lercher, J. Catal. 269 (2010) 411.
[13] R.R. Davda, J.W. Shabaker, G.W. Huber, R.D. Cortright, J.A. Dumesic, Appl. Catal. B 56 (2005) 171.
[14] P.D. Vaidya, A.E. Rodrigues, Chem. Eng. J. 117 (2006) 39.
[15] A.L. Alberton, M.M.V.M. Souza, M. Schmal, Catal. Today 123 (2007) 257.
[16] D.L. Trimm, Catal. Today 37 (1997) 233.
[17] F. Frusteri, S. Freni, V. Chiodo, L. Sparado, G. Bonura, S. Cavallaro, J. Power Sour. 132 (2004) 139.
[18] V. Klouz, V. Fierro, P. Denton, H. Katz, J.P. Lisse, S. Bouvot-Mauduit, C. Mirodatos, J. Power Sour. 105 (2002) 26.
[19] K. Takanabe, K. Aika, K. Seshan, L. Lefferts, Chem. Eng. J. 120 (2006) 133.
[20] K.O. Christensen, D. Chen, R. Lodeng, A. Holmen, Appl. Catal. A 314 (2006) 9.
[21] O. Skoplyak, M.A. Barteau, J.G. Chen, Surf. Sci. 602 (2008) 3578.
[22] D.J.M. de Vlieger, D.B. Thakur, L. Lefferts, K. Seshan, Carbon nanotubes: A promising catalyst support material for supercritical water gasification of biomass waste, ChemCatChem, Accepted for publication, doi: 10.1002/cctc.201200318.
[23] M. Osada, M. Watanabe, K. Sue, T. Adschiri, K. Arai, J. Supercrit. Fluids 28 (2004) 219.
[23] M. Osada, M. Watanabe, K. Sue, T. Adschiri, K. Arai, J. Supercrit. Fluids 28 (2004) 219.
[24] J. An, L. Bagnell, T. Cablewski, C.R. Strauss, R.W. Trainor, J. Org. Chem. 62 (1997) 2505.
[25] G.W. Huber, J.W. Shabaker, S.T. Evans, J.A. Dumesic, Appl. Catal. B 62 (2006) 226.
[26] A. Erdohelyi, J. Rasko, T. Kecskes, M. Toth, M. Dömök, K. Baan, Catal. Today 116 (2006) 367.
[27] S. Sa, H. Silva, L. Brandao, J.M. Sousa, A. Mendes, Appl. Catal. B 99 (2010) 43.
[28] S.J. Blanksby, G.B. Ellison, Acc. Chem. Res. 36 (2003) 255.
[29] B. Matas Guell, I. Babich, K. Seshan, L. Lefferts, J. Catal. 257 (2008) 229.
[30] M.M.V.M. Souza, M. Schmal, Appl. Catal. A 281 (2005) 19.
[31] X. Hu, G. Lu, Appl. Catal. B 99 (2010) 289.
[32] A.C. Basagiannis, X.E. Verykios, Appl. Catal. B 82 (2008) 77.
[33] P.E. Savage, J. Supercrit. Fluid. 47 (2009) 407.
[34] H.D. Ruan, R.L. Frost, J.T. Kloprogge, J. Raman Spectrosc. 32 (2001) 745.
[35] A.B. Kiss, G. Keresztury, L. Farkas, Spectrochim. Acta A 36 (1980) 653.
[36] R.M. Ravenelle, J.R. Copeland, W.-G. Kim, J.C. Crittenden, C. Sievers, ACS Catal. 1 (2011) 552.
[37] J.A. Yopps, D.W. Feurstenau, J. Colloid Sci. 19 (1964) 61.
[38] B. Kasprzyk-Hordern, Adv. Colloid. Interfac. 110 (2004) 19.